hydrology MDPI

Article

Hydrologic Utility of Satellite-Based and Gauge-Based Gridded Precipitation Products in the Huai Bang Sai Watershed of Northeastern Thailand

Miyuru B. Gunathilake [1,2], M. N. M. Zamri [1], Tharaka P. Alagiyawanna [1], Jayanga T. Samarasinghe [1], Pavithra K. Baddewela [3], Mukand S. Babel [4], Manoj K. Jha [5] and Upaka S. Rathnayake [1,*]

1 Department of Civil Engineering, Faculty of Engineering, Sri Lanka Institute of Technology, Colombo 10115, Sri Lanka; miyuru.g@sliit.lk (M.B.G.); en17362122@my.sliit.lk (M.N.M.Z.); en17385756@my.sliit.lk (T.P.A.); jha003@un-ihe.org (J.T.S.)
2 Central Engineering Services (Pvt) Ltd., Bauddhaloka Mawatha, Colombo 00700, Sri Lanka
3 Department of Transport and Logistics Management, Faculty of Engineering, University of Moratuwa, Colombo 10400, Sri Lanka; baddewelaswybpk.19@uom.lk
4 Department of Water Engineering and Management, Asian Institute of Technology, School of Engineering and Technology, Khlong Luang 12120, Thailand; msbabel@ait.asia
5 Department of Civil, Architectural and Environmental Engineering, North Carolina Agricultural and Technical State University, Greensboro, NC 27411, USA; mkjha@ncat.edu
* Correspondence: upaka.r@sliit.lk; Tel.: +94-71-988-3318

Citation: Gunathilake, M.B.; Zamri, M.N.M.; Alagiyawanna, T.P.; Samarasinghe, J.T.; Baddewela, P.K.; Babel, M.S.; Jha, M.K.; Rathnayake, U.S. Hydrologic Utility of Satellite-Based and Gauge-Based Gridded Precipitation Products in the Huai Bang Sai Watershed of Northeastern Thailand. *Hydrology* **2021**, *8*, 165. https://doi.org/10.3390/hydrology8040165

Academic Editor: Ranjan Sarukkalige

Received: 27 September 2021
Accepted: 1 November 2021
Published: 3 November 2021

Abstract: Accurate rainfall estimates are important in many hydrologic activities. Rainfall data are retrieved from rain gauges (RGs), satellites, radars, and re-analysis products. The accuracy of gauge-based gridded precipitation products (GbGPPs) relies on the distribution of RGs and the quality of rainfall data records obtained from these. The accuracy of satellite-based precipitation products (SbPPs) depends on many factors, including basin climatology, basin topography, precipitation mechanism, etc. The hydrologic utility of different precipitation products was examined in many developed regions; however, less focused on the developing world. The Huai Bang Sai (HBS) watershed in north-eastern Thailand is a less focused but an important catchment that significantly contributes to the water resources in Thailand. Therefore, this research presents the investigation results of the hydrologic utility of SbPPs and GbGPPs in the HBS watershed. The efficiency of nine SbPPs (including 3B42, 3B42-RT, PERSIANN, PERSIANN-CCS, PERSIANN-CDR, CHIRPS, CMORPH, IMERG, and MSWEP) and three GbGPPs (including APHRODITE_V1801, APHRODITE_V1901, and GPCC) was examined by simulating streamflow of the HBS watershed through the Soil & Water Assessment Tool (SWAT), hydrologic model. Subsequently, the streamflow simulation capacity of the hydrological model for different precipitation products was compared against observed streamflow records by using the same set of calibrated parameters used for an RG simulated scenario. The 3B42 product outperformed other SbPPS with a higher Nash–Sutcliffe Efficiency ($NSE_{monthly} > 0.55$), while APHRODITE_V1901 ($NSE_{monthly} > 0.53$) performed fairly well in the GbGPPs category with closer agreements with observed streamflow. In addition, the CMORPH precipitation product has not performed well in capturing observed rainfall and subsequently in simulating streamflow ($NSE_{monthly} < 0$) of the HBS. Furthermore, MSWEP and CHIRPS products have performed fairly well during calibration; however, they showcased a lowered performance for validation. Therefore, the results suggest that accurate precipitation data is the major governing factor in streamflow modeling performances. The research outcomes would capture the interest of all stakeholders, including farmers, meteorologists, agriculturists, river basin managers, and hydrologists for potential applications in the tropical humid regions of the world. Moreover, 3B42 and APHRODITE_V1901 precipitation products show promising prospects for the tropical humid regions of the world for hydrologic modeling and climatological studies.

Keywords: gauge-based gridded precipitation products; Huai Bang Sai (HBS) watershed; hydrologic utility; satellite-based precipitation products

1. Introduction

Precipitation is one of the major driving components of the hydrologic cycle [1]. Therefore, accurate precipitation estimates are essential for many professionals including meteorologists, hydrologists, ecologists, agriculturists, disaster management personals, energy planners, etc. for decision making and planning in various hydrologic related activities. Generally, precipitation estimates are obtained from rain gauges (RGs), meteorological radars, satellites, and re-analysis products. Technological and economic constraints limit the usage of high-tech weather radars in developing countries such as Thailand for hydrologic related applications [2]. Re-analysis data are produced through the combination of past short-range weather forecasts with observations through data assimilation. These re-analysis products can suffer from significant biases in the tropical regions [3–5]. Thus, ground-measured rainfall measurements are treated as the best for their accuracy [6]. Observed rainfall data are highly used in many hydrologic related applications. Interpolation of RG data is used to derive the gauge-based gridded precipitation products (GbGPPs). Noteworthy, dense meteorological networks are required to capture the inherent higher spatial variability of rainfall. Nevertheless, a dense meteorological network is not always possible in most regions. The Asian Precipitation Highly Resolved Observational Data Integration Towards Evaluation of Water Resources (APHRODITE) [7], Global Precipitation Climatology Center (GPCC) [8], Climate Research Unit (CRU) [9], Climate Prediction Center Global Precipitation (CPC-GP) [10] are some of the most commonly used GbGPPs in the context of water resources and climatology.

The advancements of satellites and remote sensing (RS) technologies have enabled the observation of many climatic variables (i.e., temperature, rainfall, and humidity), atmospheric parameters (i.e., aerosol content, the concentration of greenhouse gases, etc.), and terrestrial water cycles (i.e., terrestrial water storages). These satellite-based precipitation products (SbPPs) can be obtained without many disruptions, unlike the observed meteorological data. In addition, they are readily available for most of the regions of the world. More importantly, SbPPscan be extracted free of charge, which is an added advantage. Satellite technology was utilized to measure rainfall from as far as the 1970s and has achieved tremendous progress over the past few decades [11]. The Tropical Rainfall Measuring Mission (TRMM) is considered the first satellite mission, which was aimed at investigating the latent heat cycles of the tropical regions [12]. It was a joint mission between the North Atlantic Space Agency (NASA) and the Japanese Aerospace Exploration Agency (JAXA).

Precipitation Estimation based on Artificial Neural Networks techniques (PERSIANN) [13], Climate Prediction Center (CPC) MORPHing technique (CMORPH) [14], Tropical Rainfall Measuring Mission Multi-Satellite Precipitation Analysis (TMPA) products [15], Integrated MultisatellitE Retrievals for Global Precipitation Measurements (IMERG) [16], Global Satellite Mapping of Precipitation (GSMap) [17], Naval Research Laboratory developed blended-satellite precipitation technique (NRL-blend) [18], Multisource Weighted-Ensemble Precipitation (MSWEP) [19], and Climate Hazards Group InfraRed Precipitation with Station data (CHIRPS) [20] are some of the SbPPs, which cover most of the regions of the world. In addition, to the aforementioned products, some SbPPs are limited to certain regions. Rainfall Estimate (RFE) and Tropical Applications of Meteorology using SATellite, (TAMSAT v.2 and v.3) (TAMSAT), African Climatology Project (APC) v.2 [21] which cover the African continent and the Combined Scheme Approach (CoSch) [22], which cover the South American continent are few examples for region specific SbPPs.

The application of SbPPs and GbGPPs have been reported not only in hydrologic modeling [23–25] but also in many other areas including, flood inundation modeling [26], drought monitoring [27], soil erosion predictions [28], etc. Considering the diverse applications of SbPPs and GbGPPs the assessment of the efficiency of the SbPPs and GbGPPs is of extreme significance. Therefore, many hydrologic studies have been carried out by various researchers to examine the efficiency of SbPPs and GbGPPs by comparing against RGs [29–31]. Precipitation mechanism, regional and seasonal effects of climates, basin topography, and catchment size are some other important factors affecting the accuracy of SbPPs [32–35]. However, the accuracy of GbGPPs strongly relies on the reliability and the quality of the rain gauge records. Considering these facts, accuracy assessment and validation of SbPPs and GbGPPs are essential prior to decision making and many practical applications.

Although, much research has been carried out to assess the hydrologic utility of SbPPs and GbGPPs in different parts of the world, up to date, few studies have yet assessed the hydrologic utility of these in the context of Thailand. According to the best understanding of the authors of this paper, only Gunathilake et al. [2], Li et al. [36], Janjai et al. [37], Pakoksung and Takagi [38], Chokngamwong and Chiu [39], Sakolnakhon [40]; Trang et al. [41] have evaluated the efficiency of SbPPs in Thailand. Among them, only Gunathilake et al. [2], Li et al. [36], and Pakoksung and Takagi [38] have examined the hydrologic utility of SbPPs for streamflow modeling in Thailand. Nevertheless, Huai Bang Sai (HBS) watershed in the north-eastern Thailand was never examined for its hydrologic utility with SbPPs and GbGPPs. Therefore, being an important watershed in Thailand in the context of agriculture and water resources, it is highly important to assess the accuracy and efficiency of different precipitation products over the HBS watershed.

Therefore, this paper for the first time presents a comprehensive study to examine the effectiveness of nine SbPPs and three GbGPPs over the HBS watershed in north-eastern Thailand. The Soil & Water Assessment Tool (SWAT) was used to simulate streamflow in the HBS watershed using different precipitation products and to compare them against observed streamflow. The physically based and semi-distributed SWAT model has successfully been applied to simulate rainfall-runoff processes in many regions of the world. This model has been applied to simulate streamflow [42–44], examine land-use change effect on streamflow [45], evaluate the impact of climate change on streamflow [46], assess the water balance [47], model water qualities in streams [48], predict streamflow in ungauged catchments [49], etc. Therefore, the SWAT model holds a successful record of wide applications across the world, and its usage in the HBS watershed of Thailand is justifiable.

Importantly, the north-eastern part of Thailand is world-famous for its rice production and it is also a leading exporter of rice [50]. Thailand's agriculture is heavily driven by rainfall [39]. Hence, the results of this research study will be valuable to water resources planners, agriculturists, and various stakeholders (including farmers) for decision-making purposes to obtain sustainable water usage. In addition, the study provides valuable feedback to algorithm developers to improve data retrieval algorithms of SbPPs and interpolation techniques adopted in GbGPPs in the tropical humid regions of the world.

2. Materials and Methods

2.1. Study Area

The HBS watershed is in the north-eastern part of Thailand (refer to Figure 1). The HBS is a sub-watershed with a drainage area of 1340 km^2) of the greater Mekong River [51]. Figure 1 showcases the location map of the HBS, rainfall gauging stations, streamflow gauging station, and the drainage network. The sub-watershed receives an average annual rainfall of 1340 mm [52] and receives rainfall mainly during two monsoon seasons, which are the southwest monsoon (from May to October) and the northeast monsoon (from November to March). These two monsoon seasons are separated by two inter-monsoonal periods. Nevertheless, the southwest monsoon brings a significant amount of rainfall to the HBS watershed [53]. The potential evapotranspiration in the northeast region is around 1600 mm per year [36]. The weather is dry and cool during the northeast monsoon season. The temperatures are usually higher in April and May [53].

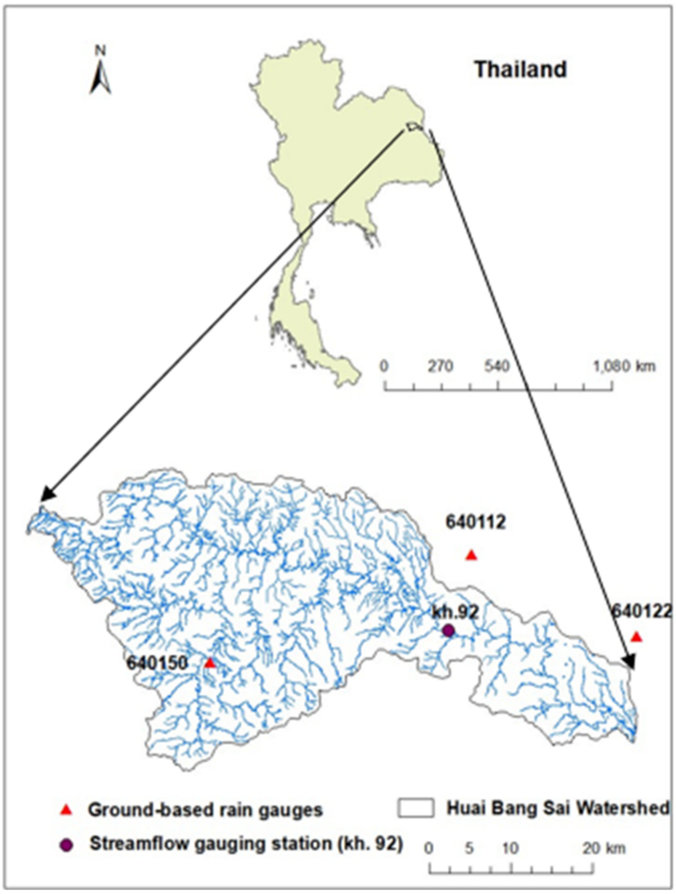

Figure 1. Hydro-meteorological network and stream network in the HBS watershed.

2.2. Obtained data

Daily observed rainfall data (for 2004–2014) at three stations with station IDs 640112 (A. Dong Luang), 640122 (A. Wan Yai), and 640150 (A. Huai Ta Poe) were collected from the Royal Irrigation Department (RID) of Thailand. In addition, daily observed streamflow data at 'Station kh.92' (Ban Kan Luang Dong, Dong Luang), draining an area of 1118 km^2 (for 2007–2014), were also obtained from the RID. The drainage map of the HBS was collected from the Deutsche Gesellschaft für Internationale Zusammenarbeit (GIZ) office in Thailand. These stations and the drainage map are shown in Figure 1.

Figure 2a–c illustrate the topography (through the Digital Elevation Model), land-use, and soil cover of the HBS watershed. The Digital Elevation Model (DEM) of a 30 m × 30 m resolution was downloaded from the United States Geological Survey website accessible through https://earthexplorer.usgs.gov/ (accessed on 25 September 2020) (refer to Figure 2a). In addition, the land-use data of 500 m resolution and scale of 1:50,000 and soil cover maps with 1 km resolution and scale of 1:100,000 for the year 2015 were obtained from the Land Development Department (LDD) of Thailand (refer to Figure 2b,c). The elevation of the watershed ranges from 0 to 636 m above mean sea level. The main land-use types of the study area are deciduous forests, cassava, and rubber plantations, which cover nearly 67%, 13%, and 6% of the land area, respectively. Most of the land in HBS is covered by Hang Chat, which has a loamy sand texture.

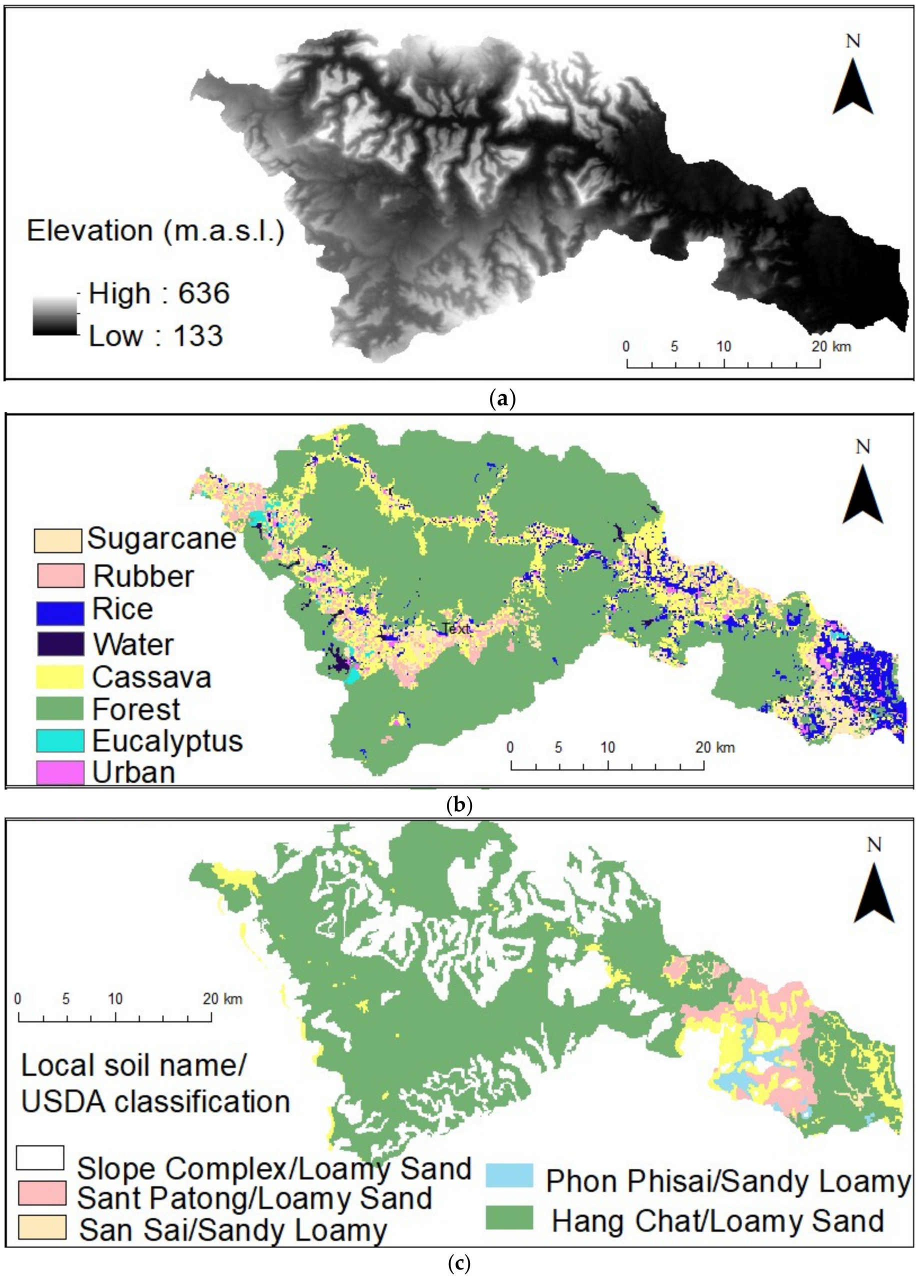

Figure 2. Details of the HBS watershed (**a**) Digital elevation model; (**b**) Land-use patterns; (**c**) Soil cover.

2.3. Satellite-Based Precipitation Products (SbPPs) and Ground-Based Gridded Precipitation Products (GbGPPs)

Table 1 provides the information of SbPPs and GbGPPs used in this study. PERSIANN products are available through https://chrsdata.eng.uci.edu/ (Accessed on 15 September 2020) whereas the TRMM products including TMPA-3B42 (version 7), TMPA-RT (version 7) and IMERG (version 6B) products are available from https://disc.gsfc.nasa.gov/ (Accessed on 20 September 2020). In addition, MSWEP (version 1.1) is available from http://www.gloh2o.org/ (Accessed on 25 September 2020). Furthermore, three GbGPPS, APHRODITE-products (version 1801 and version 1901), and GPCC (version 1) are accessible through http://aphrodite.st.hirosaki-u.ac.jp/products.html (Accessed on 25 September 2020) and https://climatedataguide.ucar.edu/climate-data/gpcc-global-precipitation-climatology-centre (Accessed on 25 September 2020) respectively.

Table 1. Description of the precipitation products.

Types	Product	Temporal Coverage	Finest Temporal Frequency	Spatial Coverage	Spatial Resolution	References
SbPPs	PERSIANN	03/2000 to date	1 h	60° N–60° S	0.25° × 0.25°	Nguyen et al. [13]
	PERSIANN-CSS	2003 to date	1 h	60° N–60° S	0.04° × 0.04°	Nguyen et al. [13]
	PERSIANN-CDR	1983 to date	1 day	60° N–60° S	0.25° × 0.25°	Nguyen et al. [13]
	TMPA-3B42	1998 to 12/2019	3 h	50° N–50° S	0.25° × 0.25°	Huffman et al. [16]
	TMPA-3B42RT	03/2000 to 12/2019	3 h	60° N–60° S	0.25° × 0.25°	Huffman & Bolvin [15]
	IMERG	03/2000 to present	30 min	90° N–90° S	0.10° × 0.10°	Huffman et al. [16]
	MSWEP	1979 to present	3 h	Global	0.25° × 0.25°	Beck et al. [19]
	CMORPH	2002 to present	30 min	60° N–60° S	0.027° × 0.027°	Joyce et al. [14]
	CHIRPS	1981 to date	Daily	50° N–50° S	0.05° × 0.05°	Funk et al. [20]
GbGPPs	GPCC	1988 to present	1 day	Global	1.0° × 1.0°	Schröder et al. [54]
	APHRODITE-V_1801	1988 to 2015	1 day	Monsoon Asia	0.25° × 0.25°	*Maeda* et al. [55]
	APHRODITE-V_1901	1988 to 2015	1 day	Monsoon Asia	0.05° × 0.05°	*Maeda* et al. [55]

2.4. SWAT Model Description

The Soil and Water Assessment Tool (SWAT) model [56] was developed by the Agriculture Research Services Division of the United States Department of Agriculture. The user-friendly Geographical Information System interface, robust algorithms to simulate hydrologic processes, and availability in the public domain are some of the attractive features of the SWAT model.

The model uses the water balance equation (which is given in Equation (1)) to simulate hydrologic processes.

$$SW_t = SW_0 + \sum_{i=1}^{t} (R_i - Q_i - ET_i - P_i - QR_i) \quad (1)$$

where SW_t and SW_o are the final and initial water content (in mm) for a period of t in days. R_i, Q_i, ET_i, P_i and QR_i are the precipitation, surface runoff, evapotranspiration, amount of water entering the vadose zone from the soil profile, and the amount of return flow on a particular day i and measured in mm. More details on the SWAT model can be found in Arnold et al. [56].

2.5. Overall Methodology

2.5.1. Extraction of SbPPs and GbGPPs

The nine satellite precipitation products used in this study were extracted through different methods. PERSIANN group of products were directly obtained from the Center for Hydrometeorology and Remote Sensing (CHRS) in CSV file format. IMERG and TRMM products were obtained as NetCDF files from National Aeronautics and Space Administration, U.S.A. (NASA) GESDISC portal. Afterwards, IMERG was extracted through the process of merging the files in Climate Data Operator (CDO) followed by the extraction using R coding in RStudio. Finally, the TRMM products were merged together, using a similar approach to IMERG. However, the extraction of the point rainfall data was carried out using MATLAB. Furthermore, GPCC, APHODITE_V1801 and APHRODITE_V1901 were extracted as NetCDF file format.

2.5.2. Watershed Model Development

The SWAT Calibration and Uncertainty Procedures (SWAT-CUP) [57] was initially used to conduct a sensitivity analysis of the model's parameters in the study area, followed by manual calibration and validation of the model for runoff. The SWAT 2012 version was used in the present study to simulate streamflow of the HBS watershed. The HBS was delineated into seven sub-watersheds and a total of 797 Hydrologic Response Units (HRUs) were created. The first three years (2004–2007) of the simulation period were treated as a warmup period in order to equilibrate between various water storages in the hydrological cycle. The streamflow gauging station kh.92 was used for calibration and validation of streamflow. The calibration period was 2007–2010 (4 years), while the validation period was 2011–2014 (4 years). In the SWAT model developed in this study, surface runoff was predicted by the Soil Conservation Service Curve Number (SCS-CN) method and potential evapotranspiration by the Hargreaves method. Detailed information on SWAT model development is explained in detail through Babel et al. [58]. The SOL_AWC factor that controls the available soil water capacity. The ESCO factor, a parameter which controls depth distribution to meet the soil evaporative demand to account for the effects of capillary action. Groundwater flow-related sensitive parameters were GW_REVAP, ALPHA_BF, GW_DELAY, and GWQMN. GW_REVAP allows water to move to the overlying saturated/vadose zone from the underlying aquifer. Similarly, model parameter GW_DELAY controls the delay between water entering the soil profile and entering the underlying aquifer. GWQMN is the threshold depth of water in a shallow aquifer required for return flow to occur. Table 2 provides the adjusted range of parameters for streamflow calibration and their final values in the Huai Bang Sai River Basin.

Table 2. Adjusted range of parameters for streamflow calibration and their final values in the HBS [58].

Rank	Parameter	Description	Initial Values	Fitted Value
1	CN	SCS-CN	73–92	
		Deciduous forest	77	73
		Cassava	85	83
		Sugarcane	85	83
		Rice	81	81
		Rubber	77	77
		Rangeland	79	79
		Water	92	92
		Urban	90	90
2	ESCO	Soil evaporation compensation factor	0.95	0.70–0.95
3	SOL_AWC	Available soil water capacity		
		Hang Chat/Loamy sand	0.14	0.1
		Slope Complex/Loamy sand	0.14	0.1
		San Sai/Sandy loamy	0.1	0.13
		Phon Phisai/Sandy loamy	0.1	0.14
		San Patong/Loamy sand	0.1	0.15
4	ALPHA_BF	Base-flow alpha factor	0.048	0.99
5	GW_DELAY	Ground water delay	31	2
6	GW_REVAP	Groundwater "revap" coefficient	0.02	0.19

The hydrograph obtained during calibration and validation was extracted from Babel et al. [58] and presented here to showcase the accuracy of the developed SWAT model (refer to Figure 3). The statistical indicators used to evaluate the hydrologic model performance were the Coefficient of Determination (R^2) and the Nash–Sutcliffe Efficiency (NSE). Acceptable accuracy can be seen from the developed model (R^2 = 0.83 and NSE = 0.82 during calibration period and R^2 = 0.78 and NSE = 0.77 during validation period). These accuracies are acceptable and reasonable in hydrologic model simulations [59].

2.5.3. Streamflow Simulation

The SbPPs and GbGPPs for this study were selected based on their performance in previous applications over the Southeast Asian Region [2,36,41]. Initially, the SWAT model developed for the HBS watershed was run with RG measured rainfall. Next, the HBS watershed was modelled with different meteorological inputs of SbPPs and GbGPPs for a time period of 11 years from 2004 to 2014. The streamflow was simulated at Station kh.92 for different precipitation inputs and compared against the observed flow data. The same parameters calibrated with RG measured rainfall were used to simulate the SWAT model with other precipitation products as well. The hydrologic utility of different precipitation products was analysed based on these results.

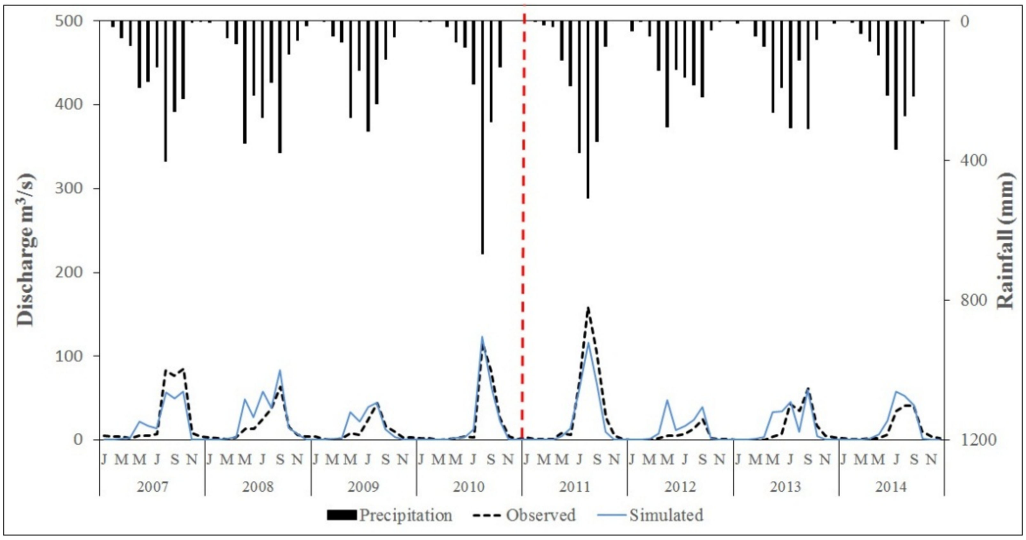

Figure 3. Hydrograph obtained during calibration (2007 to 2010) and validation (2011 to 2014) at kh.92 [58].

2.5.4. Hydrologic Performance of the Developed Models

The hydrologic performance, accuracy, and efficiency of the developed models were assessed based on the streamflow rates. These discharges were simulated based on different SbPPs, and GbGPPs were compared against the observed streamflow. The accuracy of the simulated discharge was found based on the Coefficient of Determination (R^2) and the Nash–Sutcliffe Efficiency (NSE). The mathematical formulations for R^2 and NSE are given in Equations (2) and (3), respectively.

$$R^2 = \left[\frac{\sum_{i=1}^{n} (O_i - O_{mean}) \times (S_i - S_{mean})}{\sqrt{\sum_{i=1}^{n} (O_i - O_{mean})^2 \times \sum_{i=1}^{n} (S_i - S_{mean})^2}} \right]^2 \quad (2)$$

$$NSE = 1 - \left(\frac{\sum_{i=1}^{n} (S_i - O_i)^2}{\sum_{i=1}^{n} (O_i - O_{mean})^2} \right) \quad (3)$$

where O_i stands for observed while S_i stands for simulated discharges. O_{mean} and S_{mean} stands for average of observed flow and simulated flow, respectively.

3. Results and Discussion

3.1. Comparison of Rainfall from Rain Gauges and Other Precipitation Products

Figure 4 illustrates the comparison of observed rainfall against the different precipitation products for the three stations. The dashed lines in the annual series are the extracted precipitation products, whereas the straight lines (blue coloured) are the observed annual rainfall in respective stations. The rainfall patterns are somewhat matching to each other in a particular year. The peaks and troughs are somewhat coinciding with each other for different precipitation products. However, a perfect match is not visible. Therefore, it justifies the requirement of this research in order to identify better precipitation products in the absence of observed rainfall records.

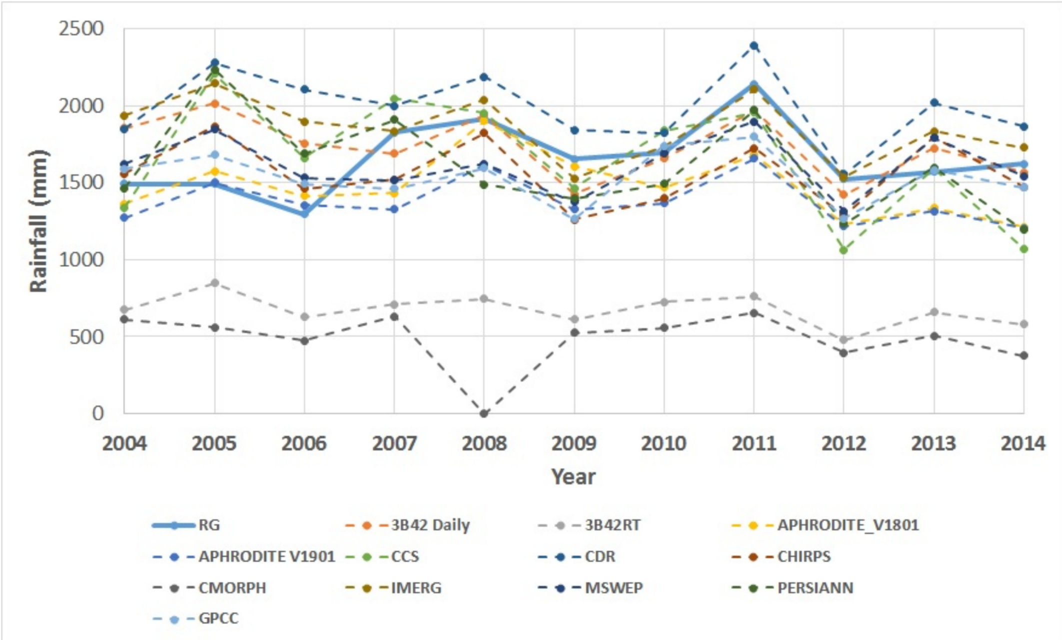

Annual precipitation

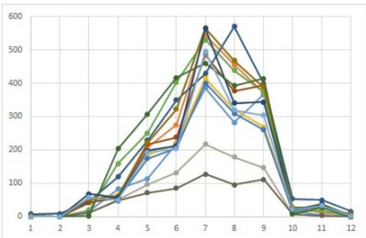

For 2005

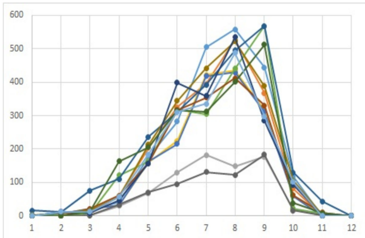

For 2011

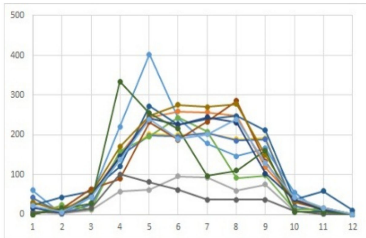

For 2012

(**a**)

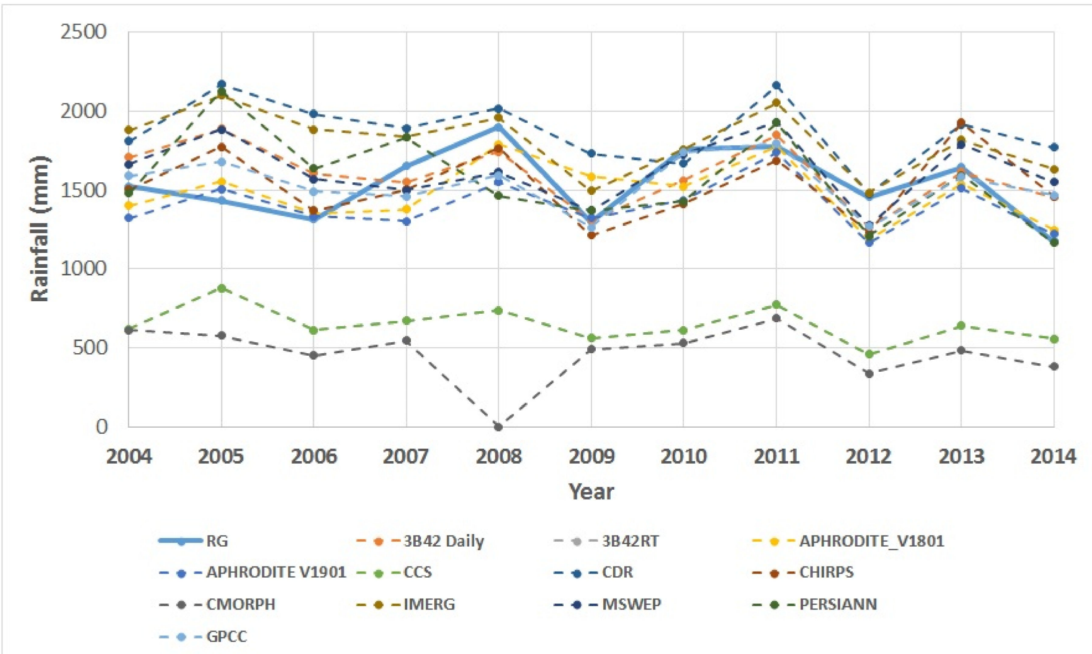

Annual precipitation

Figure 4. *Cont.*

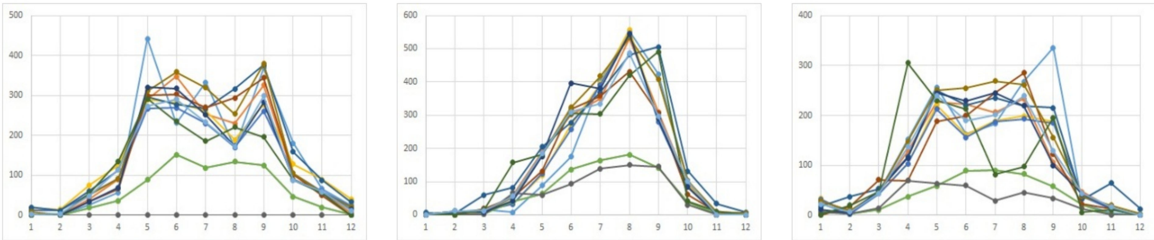

For 2008 For 2011 For 2012

(**b**)

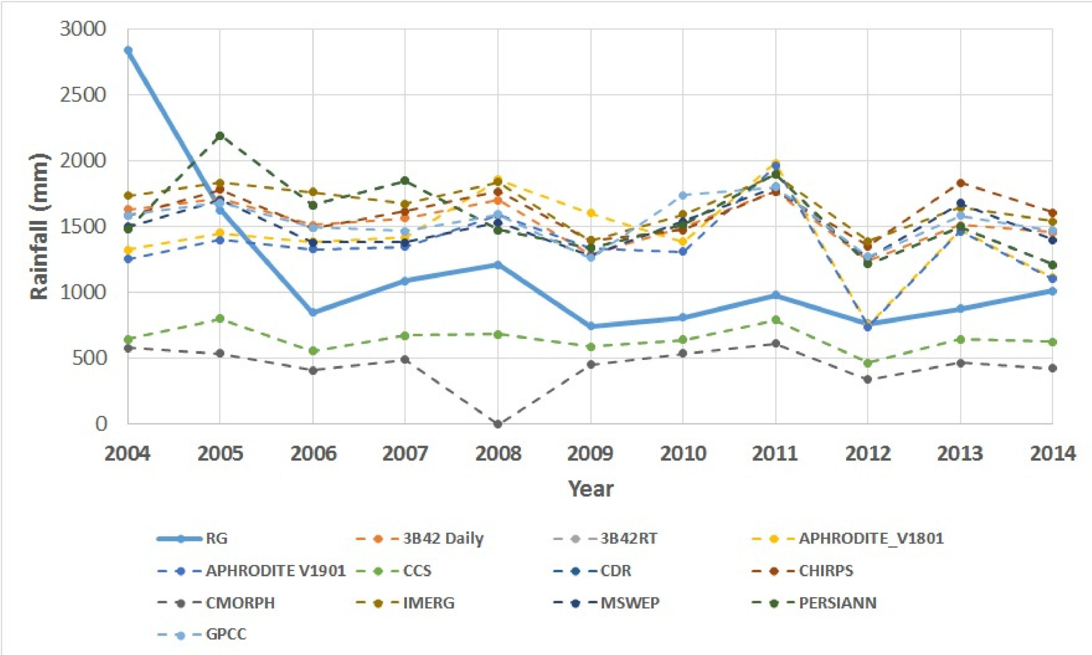

Annual precipitation

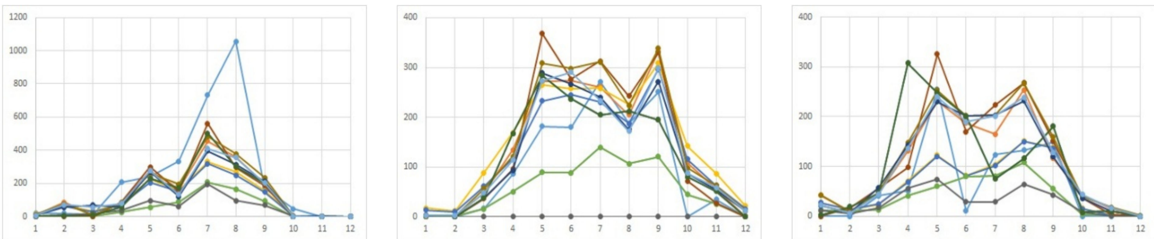

For 2004 For 2008 For 2012

(**c**)

Figure 4. Annual and monthly rainfall of different precipitation products. (**a**) For station 640112; (**b**) For station 640122; (**c**) For station 640150.

In addition, monthly variations of precipitation products for selected years are given for each station. The years 2005, 2011, and 2012 are selected for station 640112 deepening on the peaks and trough of the annual precipitations. Similarly, three years are presented for their monthly precipitation variation for 640122 and 640150 stations.

The 3B42-RT and CMORPH precipitation products under-estimated the actual annual rainfall for the 640112 station. However, other precipitation products can be seen around the observed rainfall variation. The same pattern can be seen for 640122 and 640150 stations: however, with CCS and CMORPH precipitation products. The patterns of 3B42-RT and CMORPH in 640112 are merely the same with patterns of CCS and CMORPH in 640122 and 640150 stations; however, the numerical values are different from each other. In addition, these underestimations can be clearly seen in monthly precipitation variations. Therefore, the underestimations demonstrated by 3B42-RT, CCS, and CMOPRH depict that they are incapable of simulating high rainfall events that occurred during the rainy season. Interestingly, the precipitation products other than CCS and CMORPH, overestimated the observed rainfall. Nevertheless, while considering the highly variable nature of rainfall, these precipitation products can be used for hydrological analysis.

A previous study by Li et al. [36] showed that 3B42 and IMERG over-estimates RG measured rainfall over the Chi River Basin of the north-eastern part of Thailand. The results are somewhat similar to the results obtained in the present study. Overall, it can be observed that with over-estimations and underestimations, the different precipitation products can still capture the rainfall pattern of the area.

In previous studies in the tropical humid Ethiopia the CMORPH product has also demonstrated significant underestimates [60]. The reason for this is that CMORPH precipitation estimates are derived from the microwave data exclusively. In addition to CMORPH, the CCS has also demonstrated significant underestimates over the tropical humid regions. Both observations might be due to the difficulty in detecting rainfall over the comparatively shallow convective clouds. In another study, it has been demonstrated that CMORPH has demonstrated underestimates rainfall in the Upper Haihe River Basin which has a transitional area of the humid zone to the semi-arid zone [61]. Yang et al. [62] also obtained underestimates of CMORPH rainfall over the middle part of the Haihe River Basin. The performance of CMORPH from previous studies clearly depicts that CMORPH under-estimate RG measured rainfall over the tropical humid climatic zones.

3.2. Evaluation of Streamflow Simulation Capacity of Different Precipitation Products

Figure 5 presents the simulated hydrographs for different precipitation scenarios. Figure 5a illustrates the hydrograph obtained from the hydrologic model simulated under the observed rainfall. However, there are some mismatches between observed and simulated streamflow with mixed results (over-estimations and under-estimations). These differences can clearly be seen for flood peaks during the rainy seasons. However, it is noteworthy, the flood peak in 2010 simulated by the SWAT model from RGs was comparable with observed discharge. Through eyeball analysis, it is evident that baseflow during the dry seasons in most of the years was simulated fairly well through the SWAT model. Figure 5b–d present the hydrographs obtained under the SbPPs. Fairly acceptable matches in discharges are found in Figure 5b for 3B42 precipitation product; however, underestimations in simulated discharges can be clearly seen in Figure 5c,d for 3B42-RT and CMORPH precipitation products. These two SbPPs have underestimated the precipitation too (refer to Figure 4). Figure 5e,f present the simulated hydrographs under the GbGPPs (APHRODITE_V1901 and GPCC, respectively). Over-estimations can be clearly seen in APHRODITE_V1901 and GPCC precipitation products. All other simulated hydrographs are presented in Figure A1a–g in the Appendix A of this paper. However, among all precipitation products, the RG simulated SWAT model outperformed all other precipitation products. This observation can be seen from by Li et al. [36] for the Chi River Basin in the north-eastern part of Thailand.

Conclusions drafted from Figure 5 are based on the visual observations. Therefore, the hydrologic performance of different precipitation products was examined by statistical indices, including the NSE and the R^2, which were recommended by Moriasai et al. [59]. Table 3 provides the NSE and R^2 obtained for hydrologic simulations under different precipitation products.

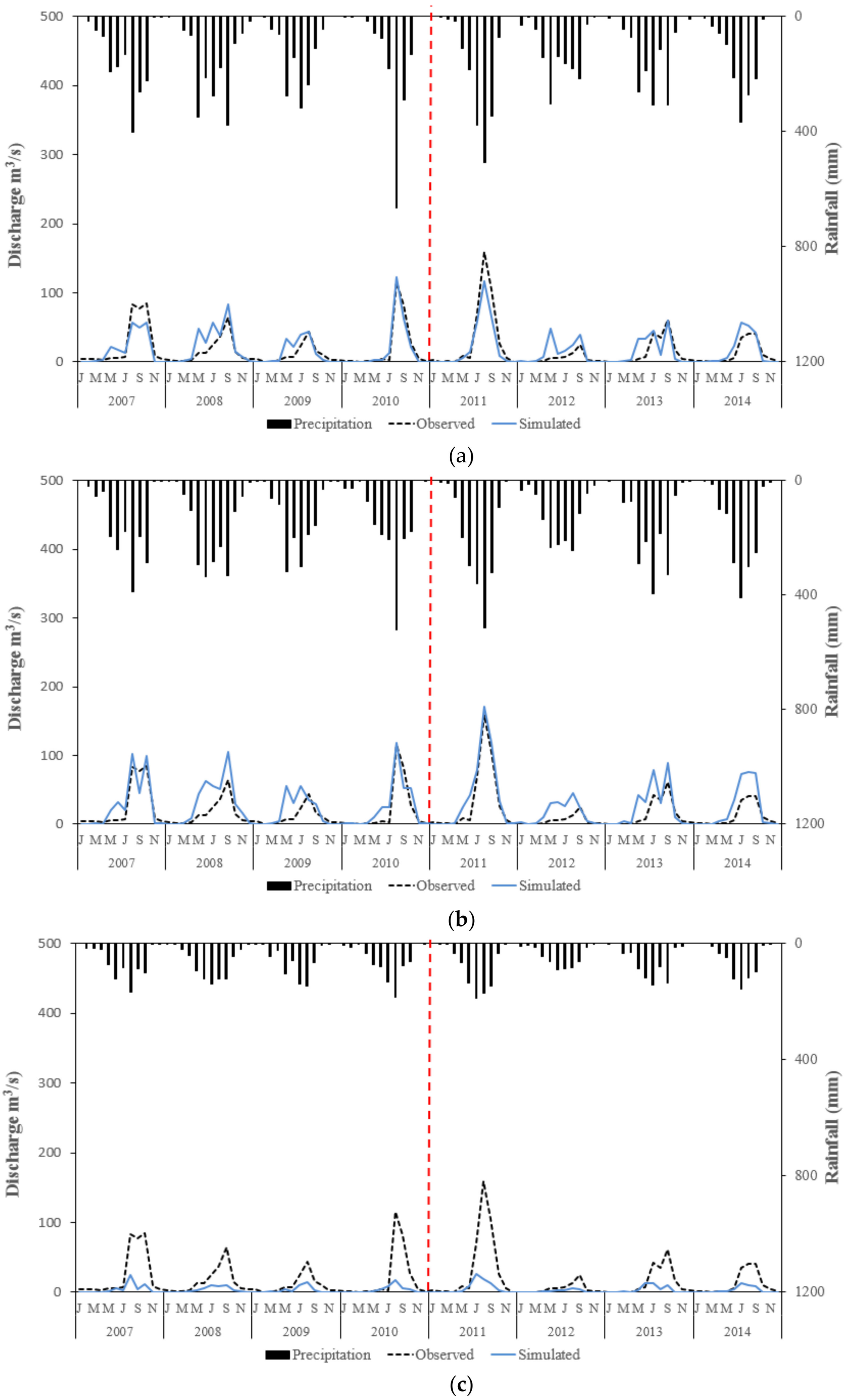

Figure 5. *Cont.*

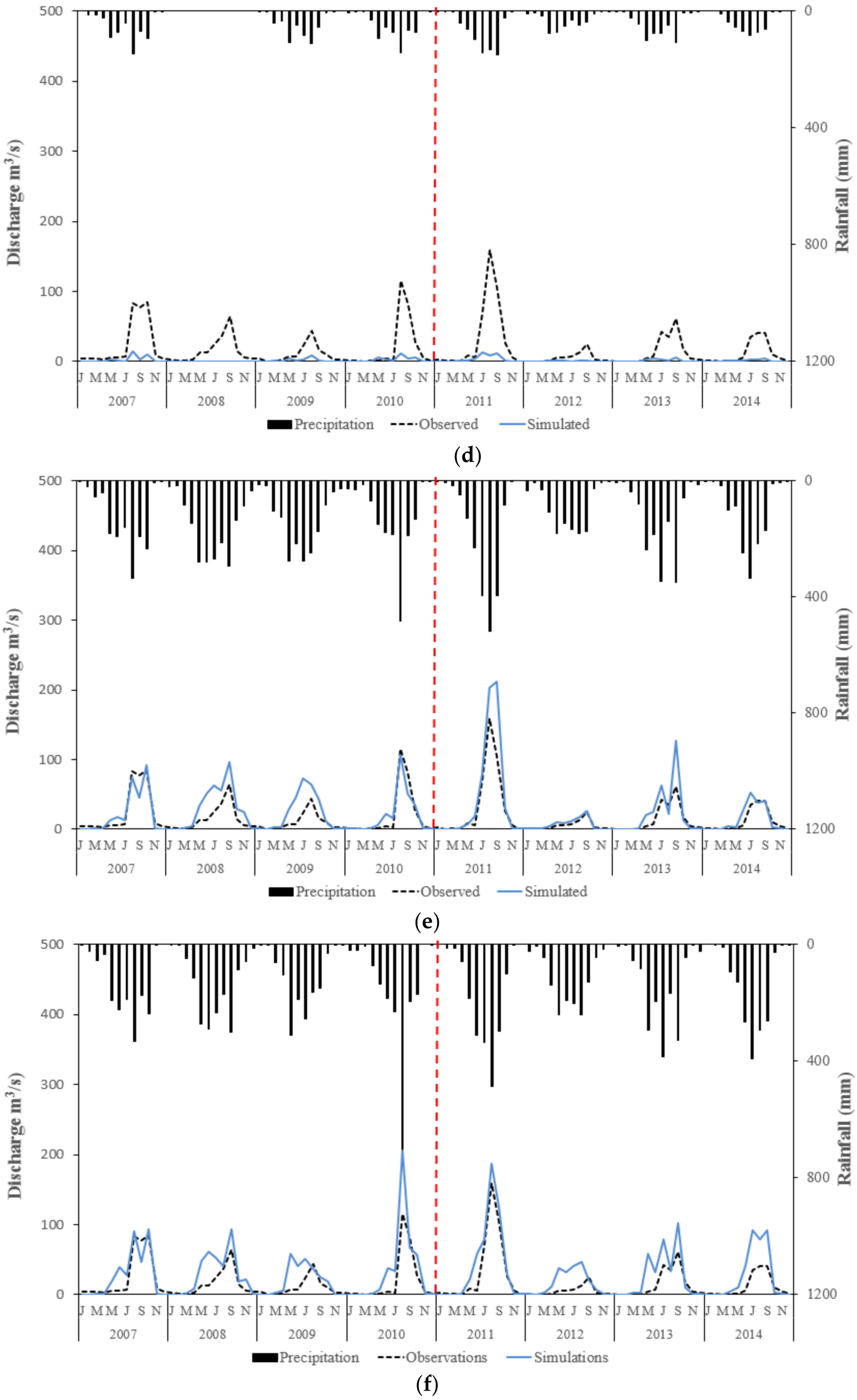

Figure 5. Simulated hydrographs under SbPPS and GbGPPs. (**a**) For observed rainfall; (**b**) For 3B42; (**c**) For 3B42-RT; (**d**) For CMORPH; (**e**) For APHRODITE V1901; (**f**) For GPCC.

Table 3. Hydrologic performance of different precipitation products.

Precipitation Product	For Calibration (2007–2010) NSE	R^2	For Validation (2011–2014) NSE	R^2
Rain gauge	0.82	0.83	0.77	0.78
PERSIANN	0.19	0.49	0.50	0.73
CCS	0.27	0.57	0.35	0.76
CDR	0.15	0.60	0.40	0.81
3B42	0.55	0.72	0.68	0.85
TMPA-3B42RT	0.01	0.63	0.10	0.62
IMERG	0.08	0.74	0.13	0.82
MSWEP	0.55	0.75	0.30	0.77
CHIRPS	0.55	0.69	0.14	0.61
CMORPH	−0.17	0.53	-0.07	0.68
APHRODITE_V1901	0.61	0.72	0.53	0.91
APHRODIE_V1801	0.21	0.66	0.49	0.90
GPCC	0.32	0.73	0.45	0.81

Among the tested precipitation products, only observed rainfall, 3B42, and APHRODITE_V1901 show NSE and R^2 values higher than 0.50 in both calibration and validation processes. Therefore, it can be argued that only these precipitation products are acceptable for hydrologic modeling of the HBS. Thus, it can be stated that 3B42 precipitation product outperformed the other SbPPs in terms of the SWAT model performance for simulating streamflow. This was observed in the obtained hydrographs (refer to Figure 4b). Similarly, APHRODITE_V1901 outperformed other GbGPPs with NSE greater than 0.50 for both calibration and validation time periods in terms of the tested GbGPPs.

Although CHIRPS and MSWEP have performed fairly well during the calibration time periods (provided with NSE values greater than 0.50), the performance of hydrologic modeling significantly decreased during the validation time period. The over-estimations compared to RGs produced from SbPPs can be the reasons for this observation. However, in contrast, PERSIANN showcased a better performance during the validation period. In addition, the CMORPH products showed the worst performance (NSE < 0) during both calibration and validation time periods. This can be directly attributed to the lower detection accuracy of rainfall events observed, which was also observed by Behrangi et al. [63].

Furthermore, CCS significantly under-estimates the streamflow from the SWAT model developed for the HBS. Similar results were demonstrated by Gunathilake et al. [2] for the Upper Nan River Basin in Northern Thailand using the Hydrologic Engineering Center-Hydrologic Modeling System (HEC-HMS) hydrologic model. The significant under-estimations of streamflow simulated by 3B42-RT, PERSIANN, and CCS were also previously demonstrated by Gunathilake et al. [2]. The underestimations of rainfall from these precipitation products can be a good reason subsequently for such underestimations in simulated streamflow. Pakoksung and Takagi [38] have also carried out hydrologic modeling for the Upper Nan River Basin using the Rainfall-Runoff Inundation Model (RRI) to simulate an extreme rainfall event. The results of the study in the Upper Nan demonstrated that the PERSIANN product significantly underestimates observed streamflow. In addition, Gunathilake et al. [64,65] showcased similar cases for the PERSIANN group of products over the Seethawaka watershed, a sub-watershed of the Kelani watershed of Sri Lanka.

Through the results of the current study, it is clear that the spatial resolution of SbPPs products does not have a clear impact on streamflow simulations. For instance, in terms of SbPPs, the TMPA-3B42 product which had the lowest spatial resolutions (0.25° × 0.25°) outperformed the CCS which had a comparatively high spatial resolution (0.04° × 0.04°). The CMORPH product which had the highest spatial resolution (0.027° × 0.027°) demonstrated the worst skills among all. Interestingly, the IMERG product which had a spatial resolution of 0.10° × 0.10° did not perform well in simulating streamflow when compared to other SbPPs (i:e PERSIANN, PERSIANN-CDR, and MSWEP) which had a comparatively lower spatial resolution (0.25° × 0.25°) to IMERG. PERSIANN, PERSIANN-CDR, MSWEP, TMPA-3B42, which had the same spatial resolution performed slightly differently in hydrologic model simulations.

However, with a slight exception, in terms of the GbGPPs, it is clear that among the GbGPPs which had the highest spatial resolution (0.05° × 0.05°), APHRODIE_V1901 outperformed two other GbGPPs in reproducing observed streamflow with NSE values greater than 0.50 for both calibration and validation time periods.

The authors of this paper believe that the uncertainties in the hydrologic model might have also induced some errors (to a certain extent). The sampling, instrumental and algorithmic errors in estimating rainfall are some of the reasons which might be attributed to the mismatches between observed and simulated streamflow. However, Tan et al. [66] demonstrated that 3B42 product has outperformed PERSIANN and CMORPH products over Malaysia. These results are comparable with the results obtained in this study for HBS watershed. Furthermore, Li et al. [38] have demonstrated that TRMM and IMERG simulated streamflow over-estimated observed streamflow in the Chi River Basin of the north-eastern part of Thailand. This observation is also similar to the present study. Therefore, the results of this presented paper are justifiable.

4. Conclusions

This study demonstrated the usefulness of satellite-based and gauge-based gridded precipitation products for hydrologic modeling in the Huai Bang Sai (HBS) watershed in north-eastern Thailand. Nine different satellite-based precipitation products (SbPPs) and three different gauged-based precipitation products (GbGPPs) were used to drive the SWAT hydrologic model for the HBS watershed. Among the analysed SbPPs, 3B42 showed promising results in terms of the hydrologic utility for the SWAT model for future applications in water resources management. In addition, among the GbGPPs, APHRODITE_V1901 can be recommended to be used for various hydrological and climatological applications in the humid tropical regions of the world. However, the differences between RG data and other different precipitation products are clearly seen through the simulated streamflow. Nevertheless, the present study provides valuable insights for water resources planners for the estimation of ecological flows. Furthermore, and more interestingly if the irrigation scheduling rules of the small tanks in the northeast part of Thailand can be incorporated into hydrologic modeling results, the modeling results can be further improved.

Through the results obtained by forcing different precipitation products into the SWAT hydrologic model, it was observed that the resolution of the product does not have a clear impact on the streamflow estimation accuracy. Hence, it can be decided that that the methods adopted in estimating precipitation in different precipitation products which will lead to accurate precipitation measurements ultimately had a clear role in hydrologic simulations. This study calls for improved hydrologic model results through bias-corrected algorithms, which can be applied for rainfall estimations. Therefore, the results of this study will be valuable for precipitation product developers to improve bias corrections in the tropical humid climates. It is expected that the evaluation and findings in this study can potentially provide useful information about SbPPs choices in terms of strengths and weaknesses and their applicability for the region. However, the application accuracy of SbPPs and GbGPPs is location specific.

Author Contributions: Conceptualization, M.B.G. and U.S.R.; methodology, M.B.G.; software, M.B.G., M.S.B., M.K.J. and J.T.S.; formal analysis, M.B.G., M.N.M.Z., T.P.A.; writing—original draft preparation, M.B.G.; writing—review and editing, J.T.S., P.K.B. and U.S.R.; visualization, M.B.G. and M.K.J.; supervision, U.S.R. All authors have read and agreed to the published version of the manuscript.

Funding: This research received no external funding.

Data Availability Statement: The climatic data used in this research study are available upon request for research purposes.

Acknowledgments: The authors of this manuscript are grateful to all data provision government agencies of Thailand including the Royal Irrigation Department (RID), Thai Meteorological Department (TMD), Land Development Department (LDD) for allowing us to carry out the work successfully. They are also thankful to all SbPPs and GbGPPs communities for making the precipitation data freely available for the international research community.

Conflicts of Interest: The authors declare no conflict of interest.

Appendix A

The following Figures are presented in support for Figure 5 in the main text.

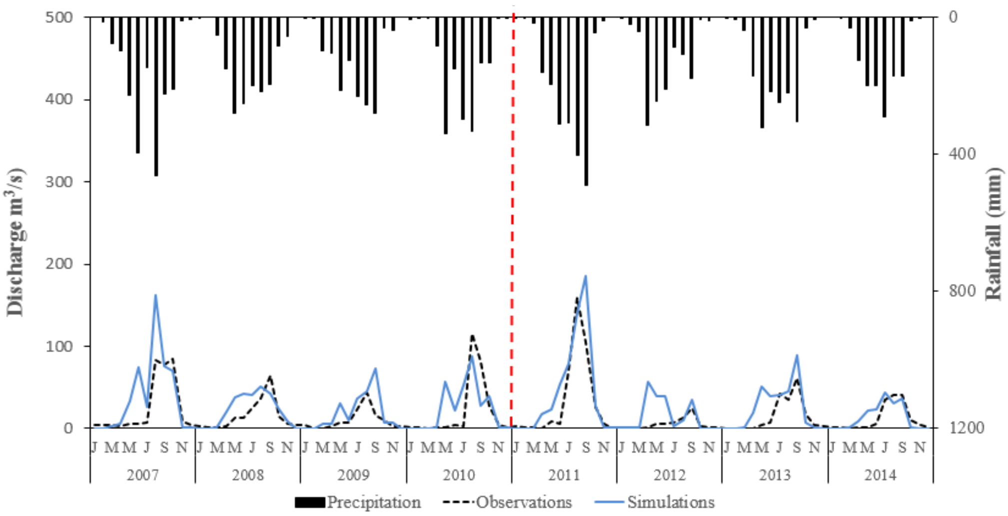

(**a**)

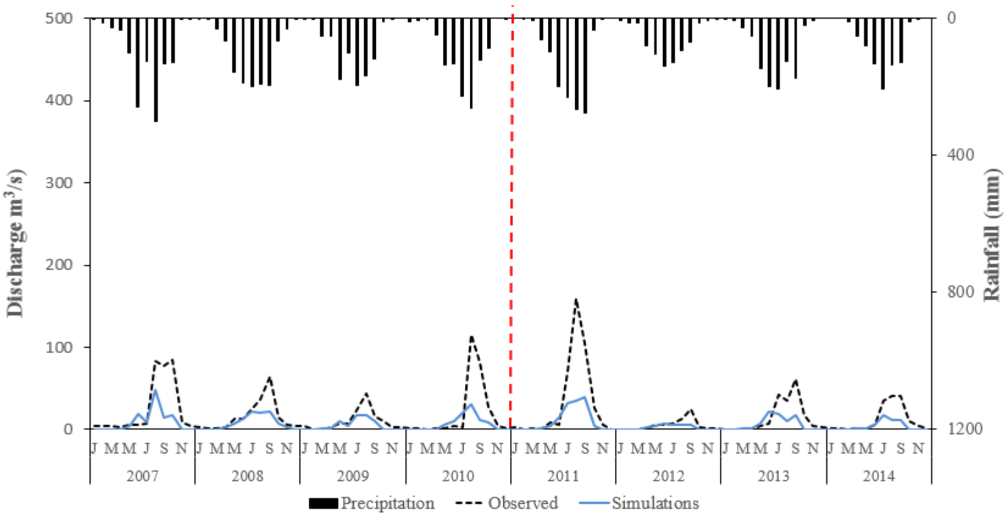

(**b**)

Figure A1. *Cont.*

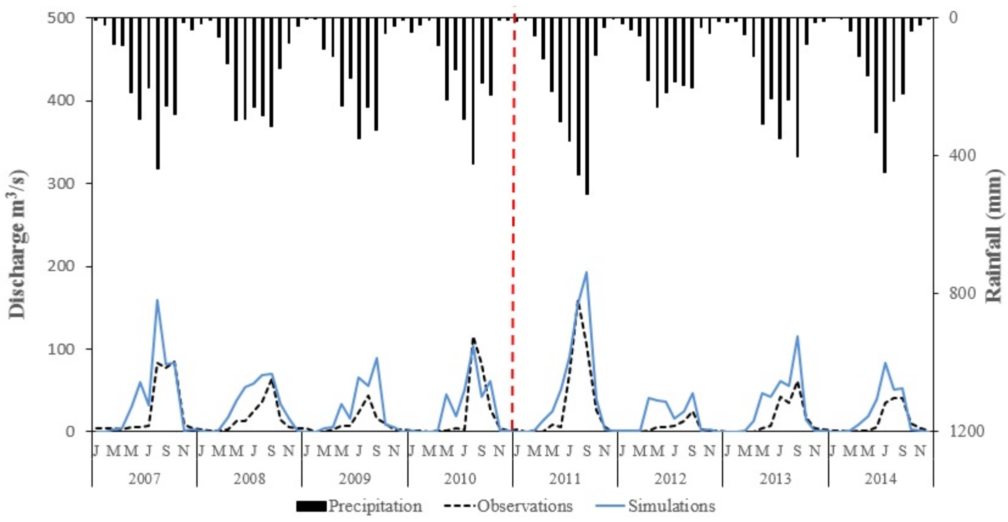

(**c**)

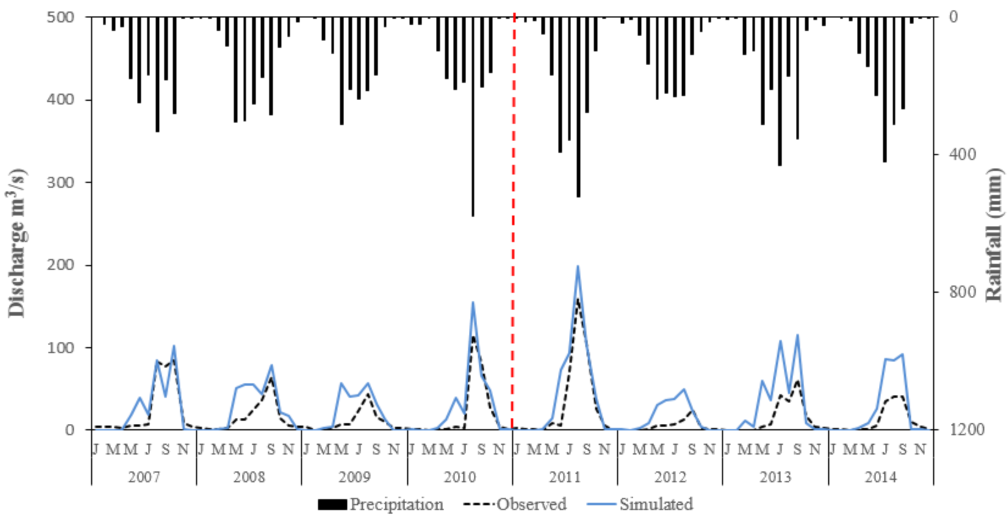

(**d**)

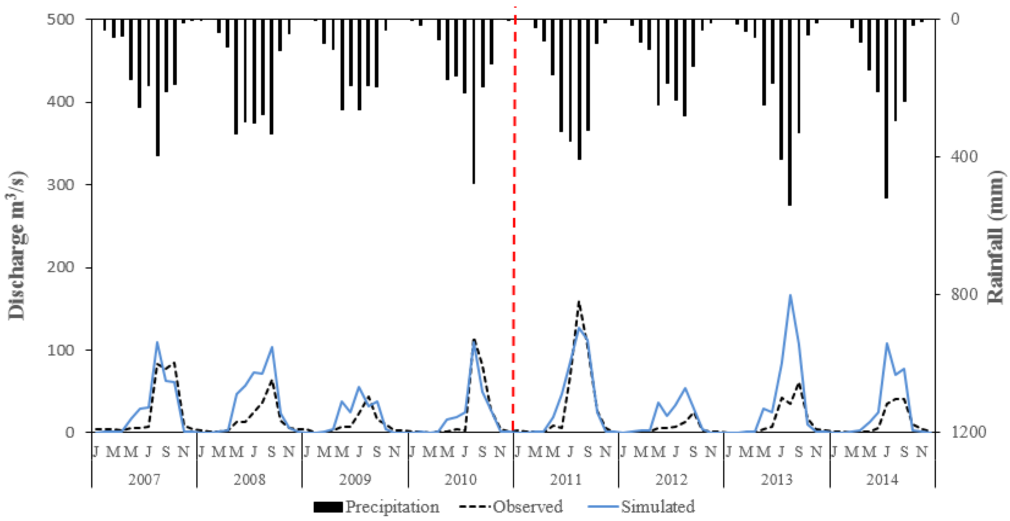

(**e**)

Figure A1. *Cont.*

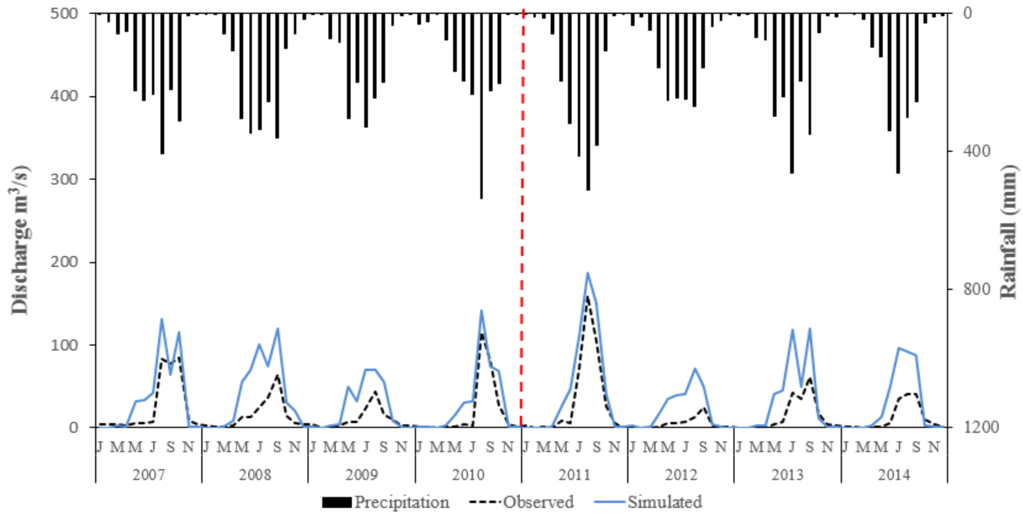

(**f**)

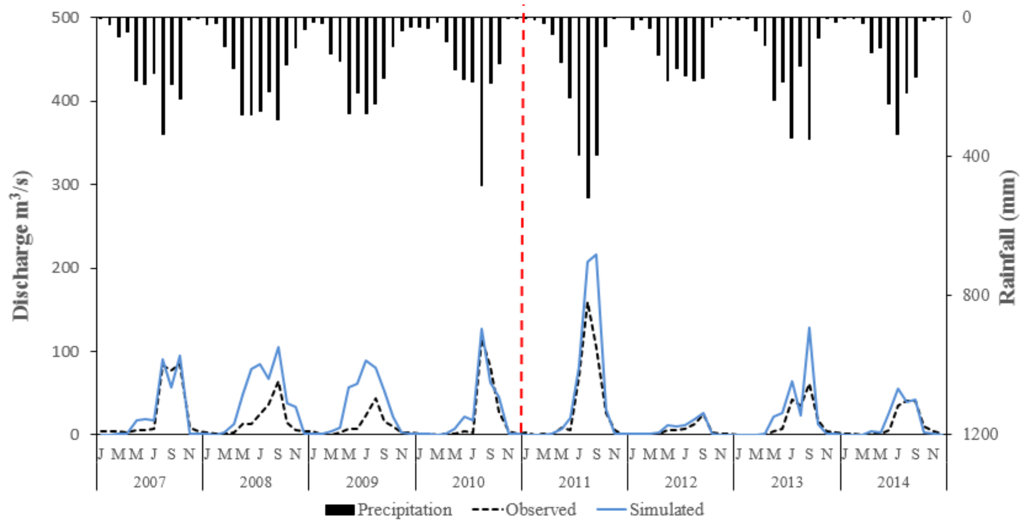

(**g**)

Figure A1. (**a**) For PERSIANN; (**b**) For CCS; (**c**) For CDR; (**d**) For MSWEP; (**e**) For CHIRPS; (**f**) For IMERG; (**g**) For APHRODITE V1801.

References

1. Alazzy, A.; Lü, H.; Chen, R.; Ali, A.; Zhu, Y.; Su, J. Evaluation Of Satellite Precipitation Products And Their Potential Influence On Hydrological Modeling Over The Ganzi River Basin Of The Tibetan Plateau. *Adv. Meteorol.* **2017**, *2017*, 3695285. [CrossRef]
2. Gunathilake, M.; Amaratunga, Y.; Perera, A.; Karunanayake, C.; Gunathilake, A.; Rathnayake, U. Statistical Evaluation And Hydrologic Simulation Capacity Of Different Satellite-Based Precipitation Products (SbPPs) In The Upper Nan River Basin, Northern Thailand. *J. Hydrol. Reg. Stud.* **2020**, *32*, 100743. [CrossRef]
3. Lorenz, C.; Kunstmann, H. The Hydrological Cycle In Three State-Of-The-Art Reanalyses: Intercomparison And Performance Analysis. *J. Hydrometeorol.* **2012**, *13*, 1397–1420. [CrossRef]
4. Trenberth, K.; Stepaniak, D.; Hurrell, J.; Fiorino, M. Quality of Reanalyses in the Tropics. *J. Clim.* **2001**, *14*, 1499–1510. [CrossRef]
5. Trenberth, K.; Fasullo, J.; Mackaro, J. Atmospheric Moisture Transports from Ocean to Land and Global Energy Flows In Reanalyses. *J. Clim.* **2011**, *24*, 4907–4924. [CrossRef]
6. Brocca, L.; Filippucci, P.; Hahn, S.; Ciabatta, L.; Massari, C.; Camici, S.; Schüller, L.; Bojkov, B.; Wagner, W. SM2RAIN–ASCAT (2007–2018): Global Daily Satellite Rainfall Data From ASCAT Soil Moisture Observations. *Earth Syst. Sci. Data* **2019**, *11*, 1583–1601. [CrossRef]
7. Yatagai, A.; Kamiguchi, K.; Arakawa, O.; Hamada, A.; Yasutomi, N.; Kitoh, A. APHRODITE: Constructing A Long-Term Daily Gridded Precipitation Dataset For Asia Based On A Dense Network Of Rain Gauges. *Bull. Am. Meteorol. Soc.* **2012**, *93*, 1401–1415. [CrossRef]

8. Schamm, K.; Ziese, M.; Becker, A.; Finger, P.; Meyer-Christoffer, A.; Schneider, U.; Schröder, M.; Stender, P. Global Gridded Precipitation Over Land: A Description Of The New GPCC First Guess Daily Product. *Earth Syst. Sci. Data* **2014**, *6*, 49–60. [CrossRef]
9. Harris, I.; Jones, P.; Osborn, T.; Lister, D. Updated High-Resolution Grids of Monthly Climatic Observations—The CRU TS3.10 Dataset. *Int. J. Climatol.* **2013**, *34*, 623–642. [CrossRef]
10. Chen, M.; Shi, W.; Xie, P.; Silva, V.; Kousky, V.; Wayne Higgins, R.; Janowiak, J. Assessing Objective Techniques For Gauge-Based Analyses Of Global Daily Precipitation. *J. Geophys. Res.* **2008**, *113*, 1–13. [CrossRef]
11. Prigent, C. Precipitation Retrieval from Space: An Overview. *Comptes Rendus Geosci.* **2010**, *342*, 380–389. [CrossRef]
12. Kummerow, C.; Barnes, W.; Kozu, T.; Shiue, J.; Simpson, J. The Tropical Rainfall Measuring Mission (TRMM) Sensor Package. *J. Atmos. Ocean. Technol.* **1998**, *15*, 809–817. [CrossRef]
13. Nguyen, P.; Ombadi, M.; Sorooshian, S.; Hsu, K.; AghaKouchak, A.; Braithwaite, D.; Ashouri, H.; Thorstensen, A. The PERSIANN Family of Global Satellite Precipitation Data: A Review and Evaluation of Products. *Hydrol. Earth Syst. Sci.* **2018**, *22*, 5801–5816. [CrossRef]
14. Joyce, R.; Janowiak, J.; Arkin, P.; Xie, P. CMORPH: A Method That Produces Global Precipitation Estimates From Passive Microwave And Infrared Data At High Spatial And Temporal Resolution. *J. Hydrometeorol.* **2004**, *5*, 487–503. [CrossRef]
15. Huffman, G.; Bolvin, D.; Nelkin, E.; Wolff, D.; Adler, R.; Gu, G.; Hong, Y.; Bowman, K.; Stocker, E. The TRMM Multisatellite Precipitation Analysis (TMPA): Quasi-Global, Multiyear, Combined-Sensor Precipitation Estimates At Fine Scales. *J. Hydrometeorol.* **2007**, *8*, 38–55. [CrossRef]
16. Huffman, G.; Bolvin, D. Real-Time TRMM Multi-Satellite Precipitation Analysis Data Set Documentation; pp. 1–48. Available online: http://trmmopen.gsfc.nasa.gov/pub/merged/V7Documents/3B4XRT_doc_V7.pdf (accessed on 20 August 2015).
17. Ushio, T.; Sasashige, K.; Kubota, T.; Shige, S.; Okamoto, K.; Aonashi, K.; Inoue, T.; Takahashi, N.; Iguchi, T.; Kachi, M.; et al. A Kalman Filter Approach to the Global Satellite Mapping of Precipitation (GSMap) from Combined Passive Microwave and Infrared Radiometric Data. *Jpn. Meteorol. Soc. Jpn.* **2009**, *87*, 137–151. [CrossRef]
18. Turk, F.; Miller, S. Toward Improved Characterization Of Remotely Sensed Precipitation Regimes with MODIS/AMSR-E Blended Data Techniques. *IEEE Trans. Geosci. Remote. Sens.* **2005**, *43*, 1059–1069. [CrossRef]
19. Beck, H.; van Dijk, A.; Levizzani, V.; Schellekens, J.; Miralles, D.; Martens, B.; de Roo, A. MSWEP: 3-Hourly 0.25° Global Gridded Precipitation (1979–2015) By Merging Gauge, Satellite, and Reanalysis Data. *Hydrol. Earth Syst. Sci.* **2017**, *21*, 589–615. [CrossRef]
20. Funk, C.; Peterson, P.; Landsfeld, M.; Pedreros, D.; Verdin, J.; Shukla, S.; Husak, G.; Rowland, J.; Harrison, L.; Hoell, A.; et al. The Climate Hazards Infrared Precipitation with Stations—A New Environmental Record For Monitoring Extremes. *Sci. Data* **2015**, *2*, 150066. [CrossRef]
21. Maidment, R.; Grimes, D.; Black, E.; Tarnavsky, E.; Young, M.; Greatrex, H.; Allan, R.; Stein, T.; Nkonde, E.; Senkunda, S.; et al. A New, Long-Term Daily Satellite-Based Rainfall Dataset for Operational Monitoring In Africa. *Sci. Data* **2017**, *4*, 17063.
22. Vila, D.; de Goncalves, L.; Toll, D.; Rozante, J. Statistical Evaluation Of Combined Daily Gauge Observations And Rainfall Satellite Estimates Over Continental South America. *J. Hydrometeorol.* **2009**, *10*, 533–543. [CrossRef]
23. Wijayarathne, D.; Coulibaly, P. Identification Of Hydrological Models For Operational Flood Forecasting In St. John'S, Newfoundland, Canada. *J. Hydrol. Reg. Stud.* **2020**, *27*, 100646. [CrossRef]
24. Habib, E.; Haile, A.; Sazib, N.; Zhang, Y.; Rientjes, T. Effect Of Bias Correction Of Satellite-Rainfall Estimates On Runoff Simulations At The Source Of The Upper Blue Nile. *Remote Sens.* **2014**, *6*, 6688–6708. [CrossRef]
25. Elgamal, A.; Reggiani, P.; Jonoski, A. Impact Analysis of Satellite Rainfall Products on Flow Simulations in the Magdalena River Basin, Colombia. *J. Hydrol. Reg. Stud.* **2017**, *9*, 85–103. [CrossRef]
26. Yoshimoto, S.; Amarnath, G. Applications of Satellite-Based Rainfall Estimates In Flood Inundation Modeling—A Case Study in Mundeni Aru River Basin, Sri Lanka. *Remote Sens.* **2017**, *9*, 998. [CrossRef]
27. Hatmoko, W.; Seizarwati, W.; Vernimmen, R. Comparison of TRMM Satellite Rainfall and APHRODITE for Drought Analysis in the Pemali-Comal River Basin. *Procedia Environ. Sci.* **2016**, *33*, 187–195.
28. Pandey, A.; Mishra, S.; Gautam, A. Soil Erosion Modeling Using Satellite Rainfall Estimates. *J. Water Resour. Hydraul. Eng.* **2015**, *4*, 318–325. [CrossRef]
29. Rozante, J.; Vila, D.; Barboza Chiquetto, J.; Fernandes, A.; Souza Alvim, D. Evaluation Of TRMM/GPM Blended Daily Products Over Brazil. *Remote Sens.* **2018**, *10*, 882. [CrossRef]
30. Ayoub, A.; Tangang, F.; Juneng, L.; Tan, M.; Chung, J. Evaluation of Gridded Precipitation Datasets in Malaysia. *Remote Sens.* **2020**, *12*, 613. [CrossRef]
31. Koutsouris, A.; Chen, D.; Lyon, S. Comparing Global Precipitation Data Sets In Eastern Africa: A Case Study of Kilombero Valley, Tanzania. *Int. J. Climatol.* **2015**, *36*, 2000–2014. [CrossRef]
32. Dinku, T.; Connor, S.J.; Ceccato, P. Comparison of CMORPH and TRMM-3B42 over Mountainous Regions of Africa and South America. In *Satellite Rainfall Applications for Surface Hydrology*; Gebremichael, M., Hossain, F., Eds.; Springer: Dordrecht, The Netherlands, 2010; pp. 193–204. [CrossRef]
33. Seibert, J.; Vis, M. Teaching Hydrological Modeling with A User-Friendly Catchment-Runoff-Model Software Package. *Hydrol. Earth Syst. Sci.* **2012**, *16*, 3315–3325. [CrossRef]
34. Sun, Q.; Miao, C.; Duan, Q.; Ashouri, H.; Sorooshian, S.; Hsu, K. A Review of Global Precipitation Data Sets: Data Sources, Estimation, and Intercomparisons. *Rev. Geophys.* **2018**, *56*, 79–107. [CrossRef]

35. Tobin, K.; Bennett, M. Using SWAT To Model Streamflow In Two River Basins with Ground And Satellite Precipitation Data. *JAWRA J. Am. Water Resour. Assoc.* **2009**, *45*, 253–271. [CrossRef]
36. Li, R.; Shi, J.; Ji, D.; Zhao, T.; Plermkamon, V.; Moukomla, S.; Kuntiyawichai, K.; Kruasilp, J. Evaluation and Hydrological Application of TRMM and GPM Precipitation Products in a Tropical Monsoon Basin of Thailand. *Water* **2019**, *11*, 818. [CrossRef]
37. Janjai, S.; Nimnuan, P.; Nunez, M.; Buntoung, S.; Cao, J. An assessment of three satellite-based precipitation data sets as applied to the Thailand region. *Phys. Geogr.* **2015**, *36*, 282–304. [CrossRef]
38. Pakoksung, K.; Takagi, M. Effect of Satellite Based Rainfall Products on River Basin Responses of Runoff Simulation on Flood Event. *Modeling Earth Syst. Environ.* **2016**, *2*, 143. [CrossRef]
39. Chokngamwong, R.; Chiu, L. Thailand Daily Rainfall and Comparison with TRMM Products. *J. Hydrometeorol.* **2008**, *9*, 256–266. [CrossRef]
40. Sakolnakhon, K. Comparison the Estimate Rainfall from Global Satellite Mapping of Precipitation (GSMaP) to Ground-based Precipitation data over Thailand. In *1st Joint Project Team Meeting for Sentinel Asia STEP3 (JPTM2013)*; Grand Millennium Hotel: Bangkok, Thailand, 2013.
41. Trang, H.T.; Manomaiphiboon, K.; Singhrattna, N.; Assareh, N. Evaluation of multiple sub-daily satellite precipitation products for Thailand. *J. Sustain. Energy Environ.* **2020**, *11*, 81–91.
42. Iresh, A.D.S.; Marasingha, A.G.N.S.; Wedanda, A.M.T.S.H.; Wickramasekara, G.P.; Wickramasooriya, M.D.J.P.; Premathilaka, M.T.C. Development of a Hydrological Model for Kala Oya Basin Using SWAT Model. *Eng. J. Inst. Eng. Sri Lanka* **2021**, *54*, 57–65. [CrossRef]
43. Hapuarachchi, P.; Zhijia, L.; Flugel, A.W. Application of the SWAT Model for River Flow Forecasting in Sri Lanka. *J. Lake Sci.* **2003**, *15*, 147–154. [CrossRef]
44. Talchabhadel, R.; Aryal, A.; Kawaike, K.; Yamanoi, K.; Nakagawa, H.; Bhatta, B.; Karki, S.; Thapa, B. Evaluation Of Precipitation Elasticity Using Precipitation Data From Ground And Satellite-Based Estimates And Watershed Modeling In Western Nepal. *J. Hydrol. Reg. Stud.* **2021**, *33*, 100768. [CrossRef]
45. Worku, T.; Khare, D.; Tripathi, S. Modeling Runoff–Sediment Response to Land Use/Land Cover Changes using Integrated GIS and SWAT Model in the Beressa Watershed. *Environ. Earth Sci.* **2017**, *76*, 550. [CrossRef]
46. Chattopadhyay, S.; Jha, M. Hydrological Response Due To Projected Climate Variability in Haw River Watershed, North Carolina, USA. *Hydrol. Sci. J.* **2016**, *61*, 495–506. [CrossRef]
47. Ayivi, F.; Jha, M. Estimation of Water Balance and Water Yield in the Reedy Fork-Buffalo Creek Watershed in North Carolina using SWAT. *Int. Soil Water Conserv. Res.* **2018**, *6*, 203–213. [CrossRef]
48. Li, M.; Guo, Q. SWAT Model Simulation of Non-Point Source Pollution in the Miyun Reservoir Watershed. *IOP Conf. Ser. Earth Environ. Sci.* **2020**, *428*, 012075. [CrossRef]
49. Warusavitharana, E. Semi-Distributed Parameter Optimization and Uncertainty Assessment for an Ungauged Catchment of Deduru Oya Basin in Sri Lanka. *Int. J. River Basin Manag.* **2019**, *18*, 95–105. [CrossRef]
50. Titapiwatanakun, B.; Titapiwatanakun, B. The Rice Situation in Thailand—TA-REG 7495. In *Support for the Association of Southeast Asian Nations Plus Three Integrated Food Security Framework*; Asian Development Bank (ADB): Mandaluyong, PH, USA, 2012; pp. 1–29.
51. Volker, A. Proceedings of the Hamburg Symposium—Publ. No. 140; International Association of Hydrological Sciences (IAHS): Hamburg, Germany, 1983; pp. 127–138.
52. Puktlang, W.; Mongkolsawat, C.; Suwanwerakamtorn, R. The Impact of Expanding Rubber Tree Plantation on Soil Erosion in the Mekong-Sub Basin. In Proceedings of the 34th Asian Conference on Remote Sensing—ACRS 2013, Bali, Indonesia, 20–24 October 2013; pp. 1–8.
53. Phien, H.; Arbhabhirama, A.; Sunchindah, A. Rainfall Distribution In Northeastern Thailand / Sur La Distribution De Pluie Dans Le Nord-Est De Thailande. *Hydrol. Sci. Bull.* **1980**, *25*, 167–182. [CrossRef]
54. Schröder, M.; Becker, A.; Dietzsch, F.; Fennig, K.; Graw, K.; Gutenstein, M.; Hollmann, R.; Niedorf, A.; Ziese, M. *HOAPS/GPCC Global Daily Precipitation Data Record with Uncertainty Estimates Using Satellite and Gauge Based Observations at 1.0°*; Deutscher Wetterdienst: Offenbach, Germany, 2019. [CrossRef]
55. Maeda, M.; Yasutomi, N.; Yatagai, A.; National Center for Atmospheric Research Staff (Eds.) The Climate Data Guide: APHRODITE: Asian Precipitation—Highly-Resolved Observational Data Integration Towards Evaluation of Water Resources. (Last Modified 29 July 2020). Available online: https://climatedataguide.ucar.edu/climate-data/aphrodite-asian-precipitation-highly-resolved-observational-data-integration-towards (accessed on 14 December 2020).
56. Arnold, J.; Srinivasan, R.; Muttiah, R.; Williams, J. Large Area Hydrologic Modeling and Assessment: Part I. Model Development. *J. Am. Water Resour. Assoc.* **1998**, *34*, 73–89. [CrossRef]
57. Abbaspour, K. *SWAT-CUP User Manual, SWAT Calibration and Uncertainty Programs*; EAWAG: Zurich, Switzerland, 2015.
58. Babel, M.S.; Gunathilake, M.B.; Jha, M.K. Evaluation of Ecosystem-based Adaptation Measures for Sediment Yield in a Tropical Watershed in Thailand. *Water* **2021**, *13*, 2767. [CrossRef]
59. Moriasi, D.; Arnold, J.; Van Liew, M.; Bingner, R.; Harmel, R.; Veith, T. Model Evaluation Guidelines for Systematic Quantification Of Accuracy In Watershed Simulations. *Trans. ASABE* **2007**, *50*, 885–900. [CrossRef]

60. Bitew, M.M.; Gabremichael, M. Evaluation through Independent Measurements: Complex Terrain and Humid Tropical Region in Ethiopia. In *Satellite Rainfall Applications for Surface Hydrology*; Gebremichael, M., Hossain, F., Eds.; Springer: Dordrecht, The Netherlands, 2010.
61. Wu, Z.; Xu, Z.; Wang, F.; He, H.; Zhou, J.; Wu, X.; Liu, Z. Hydrologic Evaluation of Multi-Source Satellite Precipitation Products for the Upper Huaihe River Basin, China. *Remote Sens.* **2018**, *10*, 840. [CrossRef]
62. Yang, X.; Yong, B.; Hong, Y.; Chen, S.; Zhang, X. Error analysis of multi-satellite precipitation estimates with an independent raingauge observation network over a medium-sized humid basin. *Hydrol. Sci. J.* **2016**, *61*, 1813–1830. [CrossRef]
63. Behrangi, A.; Khakbaz, B.; Jaw, T.; AghaKouchak, A.; Hsu, K.; Sorooshian, S. Hydrologic Evaluation Of Satellite Precipitation Products Over A Mid-Size Basin. *J. Hydrol.* **2011**, *397*, 225–237. [CrossRef]
64. Gunathilake, M.; Karunanayake, C.; Gunathilake, A.; Marasingha, N.; Samarasinghe, J.; Bandara, I.; Rathnayake, U. Hydrological Models And Artificial Neural Networks (Anns) To Simulate Streamflow In A Tropical Catchment Of Sri Lanka. *Appl. Comput. Intell. Soft Comput.* **2021**, *2021*, 6683389.
65. Gunathilake, M.; Senerath, T.; Rathnayake, U. Artificial Neural Network Based PERSIANN Data Sets In Evaluation Of Hydrologic Utility Of Precipitation Estimations In A Tropical Watershed Of Sri Lanka. *AIMS Geosci.* **2021**, *7*, 478–489. [CrossRef]
66. Tan, M.; Ibrahim, A.; Duan, Z.; Cracknell, A.; Chaplot, V. Evaluation of Six High-Resolution Satellite and Ground-Based Precipitation Products over Malaysia. *Remote Sens.* **2015**, *7*, 1504–1528. [CrossRef]